Site- and sequence-selective ultrafast hydration of DNA

Samir Kumar Pal, Liang Zhao, Tianbing Xia, and Ahmed H. Zewail*

Laboratory for Molecular Sciences, Arthur Amos Noyes Laboratory of Chemical Physics, California Institute of Technology, Pasadena, CA 91125

Contributed by Ahmed H. Zewail, September 26, 2003

Water molecules in the DNA grooves are critical for maintaining structural integrity, conformational changes, and molecular recognition. Here we report studies of site- and sequence-specific hydration dynamics, using 2-aminopurine (Ap) as the intrinsic fluorescence probe and with femtosecond resolution. The dodecamer d[CGCA(Ap)ATTTGCG]$_2$ was investigated, and we also examined the effect of a specific minor groove-binding drug, pentamidine, on hydration dynamics. Two time scales were observed: ≈1 ps (bulk-like) and 10–12 ps (weakly bound type), consistent with layer hydration observed in proteins and DNA. However, for denatured DNA, the cosolvent condition of 40% formamide hydration is very different: it becomes that of bulk (in the presence of formamide). Well known electron transfer between Ap and nearby bases in stacked assemblies becomes inefficient in the single-stranded state. The rigidity of Ap in the single strands is significantly higher than that in bulk water and that attached to deoxyribose, suggesting a unique role for the dynamics of the phosphate-sugar-base in helix formation. The disparity in minor and major groove hydration is evident because of the site selection of Ap and in the time scale observed here (in the presence and absence of the drug), which is different by a factor of 2 from that observed in the minor groove–drug recognition.

The influence of hydration on the conformation and interactions of DNA has been the subject of many investigations using x-ray crystallography, NMR, molecular dynamics, and thermodynamic techniques (for recent reviews see refs. 1–4). The important role of water in the three-dimensional structures adopted by DNA is summarized in one of these reviews (1). At the interface between DNA and proteins (5, 6), water molecules in the first hydration shell of DNA "mark" the positions where protein residues hydrogen-bond to DNA. Even for specificity of cleavage in DNA, water activity affects site-specific recognition of DNA by *Eco*RI (6) as it does in protein function (7).

In the minor groove of a B-form DNA duplex, hydration and its role in drug binding are striking. In a recent publication (8) from this laboratory, we described how the drug (Hoechst 33258) bound in the minor groove of DNA can be used to probe the dynamics of the water layer. For a DNA dodecamer duplex d(CGCAAATTTGCG)$_2$, two well separated hydration times were found: 1.4 and 19 ps, compared with 0.2 and 1.2 ps for the same drug in bulk water. For comparison, we also studied genomic calf thymus DNA for which the hydration exhibits time scales similar to those of the dodecamer DNA.

In this study, we use a DNA base analog, 2-aminopurine (Ap), in the same dodecamer B-DNA duplex d(CGCAApATTTGCG)$_2$ as an intrinsic fluorescence probe. Ap has been shown by NMR spectroscopy and thermodynamic measurements to form a stable base pair with thymine in a DNA oligomer, stabilized by two hydrogen bonds in a Watson–Crick geometry (9, 10) (see Fig. 1). Thus it is reasonable to consider that the modification by Ap does not alter the native structure of the duplex dodecamer, the x-ray structure of which has been reported already (11) (Fig. 1).

From the structural study of the dodecamer d(CGCAAATTTGCG)$_2$, it is evident that Ap is positioned at the floor wall separating two grooves (major and minor). Thus, we are able, with UV excitation, to follow its solvation in the dynamic Stokes shift, caused by water hydration on the femtosecond to picosecond time scale. We then compare the results of the dodecamer with those obtained for free Ap in bulk water (ref. 12 and references therein). To examine the change in hydration dynamics of Ap after recognition by a drug [pentamidine, which binds in the minor groove of duplexes (13, 14)], we performed another set of femtosecond studies of hydration for the Ap-modified DNA–drug complex. For comparison with single strands, we also studied the dodecamer in its denatured state in a solution of 40% formamide and the free Ap in 40% formamide aqueous solutions. For all systems studied, we measured the decay of the fluorescence anisotropy to ascertain the degree of rigidity.

Experimental Procedures

Sample Preparation. Ap (99% pure; Sigma), pentamidine as the diisothionate salt (98% pure; Sigma), formamide (99.5% pure; Merck), and deoxyribose-Ap (99% pure; Sigma) were used without further purification. The dodecamer DNA(s) with sequences 5′-CGCAAATTTGCG-3′ and 5′-CGCAApATTTGCG-3′ were synthesized by using standard phosphoramidite chemistry at the California Institute of Technology Oligo Facility. The oligonucleotides were purified with oligonucleotide purification cartridge, desalted with an NAP25 column (Amersham Pharmacia), and then quantified with UV absorbance at 260 nm. The DNA(s) was annealed (to form duplexes) by heating to 368 K for 2 min in a 0.02 M phosphate buffer (pH 7.4) in water from a Nanopure (Dubuque, IA) purification system and allowed to cool slowly. The DNA–drug (pentamidine) complex was prepared by mixing the drug (500 μM) with the Ap-modified duplex (100 μM) in the aqueous buffer with continuous stirring for 1 h. The yield of the complex was >99% (1:1 complex) at our drug concentration, based on an equilibrium constant of $\approx 10^7$ M^{-1} (15). The denaturing solution was made of 40% formamide and 60% water, without buffer salt.

Time-Resolved Studies. All the transients were obtained by using the femtosecond-resolved fluorescence up-conversion technique. A detailed experiment setup is described elsewhere (16). For the studies reported here, a femtosecond pulse (200 nJ) at 322 nm was used to excite Ap. For detection wavelength at 360–370 nm, we used excitation at 330 nm, because the peak of the Raman scattering at excitation 322 nm is at 368 nm, close to the detection at ≈360–370 nm. To obtain time-resolved anisotropy, $r(t)$, at 380 nm and to construct hydration correlation function, $C(t)$, we followed the procedure detailed in our previous work (16).

NMR Studies. One-dimensional imino proton NMR spectra were collected on Varian INOVA 600 at either 10 or 25°C in a 0.02 M phosphate buffer (pH 7.4) in $H_2O/^2H_2O$ (90:10). The concentrations of these duplexes in these experiments were ≈100 μM, similar to that used in our time-resolved measurements. Solvent suppres-

Abbreviation: Ap, 2-aminopurine.

*To whom correspondence should be addressed. E-mail: zewail@caltech.edu.

www.pnas.org/cgi/doi/10.1073/pnas.2336222100

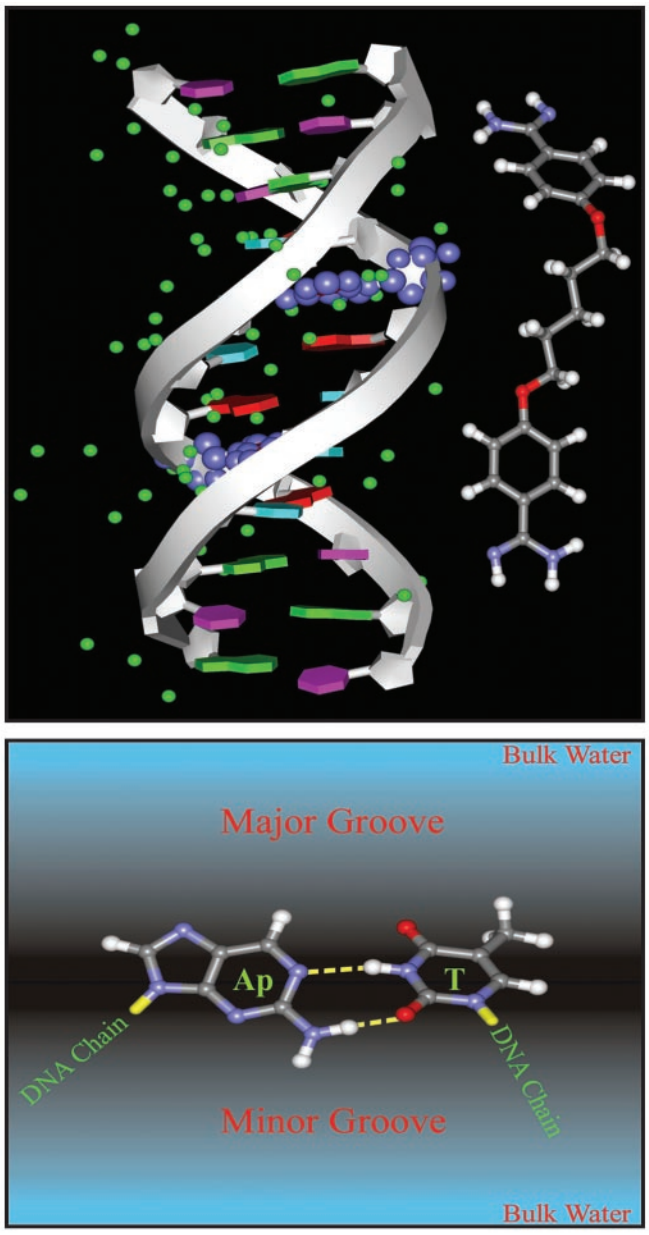

Fig. 1. (*Upper*) The x-ray structure of the dodecamer duplex DNA. The structure was downloaded from the Protein Data Bank (ID code 264D) and handled with the program WEBLAB VIEWERLITE (see ref. 11). Two of the adenine bases have been marked (blue balls) to show the sites of modification by Ap. The structure of the drug pentamidine is shown on the right. (*Lower*) Watson–Crick base pairing is shown between Ap and thymine (T). Note that our probe Ap would probe the water molecules from both grooves.

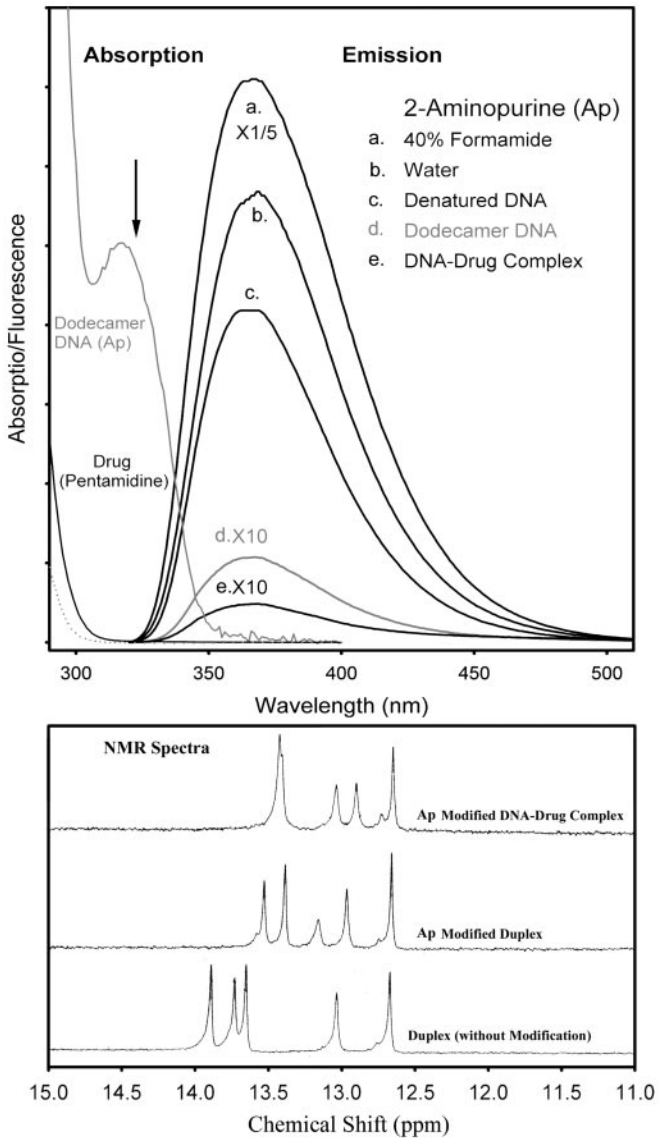

Fig. 2. (*Upper*) Steady-state fluorescence spectra of Ap in different systems. The spectra for Ap in 40% formamide, dodecamer duplex, and DNA–drug complex were multiplied by 1/5, 10, and 10, respectively. The arrow marks the excitation wavelength (322 nm). The absorption is that of DNA with Ap (gray), DNA without Ap (dotted), and free drug (black). (*Lower*) The NMR spectra of the systems studied (see text).

sion was achieved by using a modified Watergate pulse sequence. Approximately 100–200 transients were averaged.

Results and Discussion

Steady-State Optical Spectroscopy. The effect of solvation on the Ap emission (solvatochromism) has been studied (12). Ap shows red shift in its emission maximum with the increase in solvent polarity. As shown in Fig. 2, Ap in DNA has an absorption maximum at 320 nm, which is ≈15-nm red-shifted compared with that in bulk water; the dodecamer without Ap does not show the peak around 320 nm. To compare the relative intensities at emission maxima, we maintained the same optical densities of the systems used in our study at 310 nm (excitation).

In the emission spectra, Ap in bulk water and in DNA shows fluorescence maxima at 370 and 365 nm, respectively (310 nm excitation). The reason for exciting at 310 nm instead of 322 nm, which is mostly used in our time-resolved studies, is to avoid Raman scattering on top of the emission maximum (≈368 nm). The fluorescence spectra are practically independent of excitation wavelengths between 310 and 330 nm. The emission spectrum of the DNA–drug complex is not significantly different from that of DNA without drug. The black curve shows the absorption of the drug in aqueous buffer, and there is no absorption at ≈310–330 nm.

From the spectra it is evident that the emission intensity of Ap in the DNA duplex is decreased relative to that in bulk water but increased after denaturation (single-stranded). It was demonstrated (17, 18) that the main nonradiative pathway of the Ap in DNA is an electron transfer mechanism between Ap and neighboring bases. The decrease in emission intensity of Ap in DNA

duplex, as observed in our steady-state experiments, is consistent with these studies. Note the higher emission intensity of Ap in 40% formamide solution; the increase of the yield of fluorescence in the case of denatured DNA could be a combined effect of host solvent (40% formamide) and less efficient electron transfer caused by a lack of stacking in the single-stranded form, as shown below.

NMR Spectroscopy. Fig. 2 *Lower* shows the imino proton region of DNA duplex with and without the drug. As a control, the presence of five well resolved imino proton signals for unmodified DNA duplex d(CGCAAATTTGCG)$_2$ is consistent with previous literature (13, 19), and their chemical shifts agree with the reported values. Note that the signal from the terminal GC pair is missing due to fraying. For the Ap-modified DNA duplex d(CGCA<u>Ap</u>ATTTGCG)$_2$, the chemical shifts for GC base pairs are not strongly perturbed, whereas those of the AT base pairs around the Ap–T pair are upfield-shifted from the unmodified DNA, suggesting a somewhat different electronic effect by the neighboring Ap–T pair than a regular AT pair. In the presence of drug, imino protons from central AT and Ap–T base pairs show specific chemical-shift perturbation, confirming that the drug specifically interacts with the DNA duplex, particularly in the central AT and Ap–T base pair region. The GC pairs are not perturbed significantly, consistent with the literature report (19). We also studied the duplex DNA in the presence of 40% formamide and found no signals in the imino proton region, indicating complete denaturation (20) of the duplex to essentially single-stranded DNA.

Dodecamer Duplex DNA: Dynamics of Hydration. Fig. 3 *Upper* shows the femtosecond-resolved transients of Ap-modified duplex in buffer solutions with a series of systematic wavelength detection. The signal initially decays at the blue side of fluorescence but rises at the red side. In contrast, a decay component for all wavelengths was found with a time constant of ≈150 ps as shown in Fig. 3 *Upper Right*. The transients at wavelengths 430 and 440 nm show a small component (≈10%) of decays with a time constant of ≈10 ns; the fluorescence lifetime of Ap in water is 11.8 ns (21).

The hydration correlation function, $C(t)$ (Fig. 4), is a sum of two exponentials with the time constants 1.5 ps (51%) and 11.6 ps (49%); any sub-100-fs components in these dynamics are unresolved. The net spectral shift is 693 cm^{-1}. To ascertain the degree of orientational rigidity of the Ap stacked in the dodecamer duplex, we obtained the fluorescence anisotropy, $r(t)$, at 380 nm. The $r(t)$ is observed to persist at least up to 200 ps as shown in Fig. 4 *Upper Inset*. The $r(t)$ of Ap in bulk water is observed to be biexponential (see below) with time constants of 19 ps (58%) and 54 ps (42%). The dramatic lengthening of the Ap anisotropy decay in dodecamer, compared with bulk, is consistent with a rigid stacking in the DNA duplex.

The observed ≈150-ps component, which is manifested as a decay in the detected transients, is caused by charge transfer (17, 18); the radiative rate is also altered (22). A more detailed picture of the charge-transfer mechanism is discussed in refs. 17 and 18. Our measured decay of ≈150 ps is consistent with the reported decay time constant of 155 ps for DNA with adenine adjacent to Ap (17).

As solvation proceeds, the total available energy in the Ap molecule above the CT barrier decreases with time. This results in a general increase of the contribution of the CT component (and longer decay time) as the emission is monitored from the blue to the red edge. Note that the time scale of the CT dynamics (≈150 ps) is much longer than that of solvation (≈12 ps). Thus, during the transformation from initial excited state to CT state, water can "immediately" respond to the new configuration of Ap. The presence of a nanosecond component (≈10 ns) on the red edge is caused by emission from the relaxed Ap molecule at the bottom of the initial excited state and also the heterogeneity in the local structure of Ap, which results in some configurations unfavorable for CT (as discussed in ref. 17).

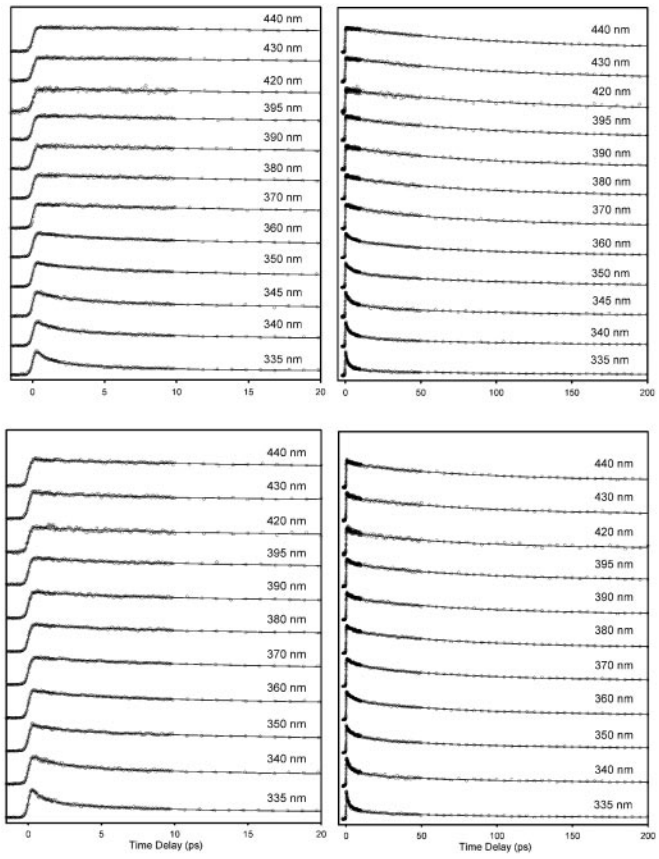

Fig. 3. Femtosecond-resolved fluorescence transients for Ap in dodecamer DNA (*Upper*) and dodecamer DNA–drug complex (*Lower*). (*Right*) The transients on longer time scales (see text).

DNA–Drug Complex. Fig. 3 *Lower* shows transients obtained from up-conversion experiments of the DNA–drug complex in aqueous buffer solutions. On the blue edge of the spectra the signals decay on different time scales depending on wavelengths, whereas on the red edge the signal is seen to rise. A decay component of time constants of ≈80 ps is present in all wavelengths detected (see Fig. 3 *Lower Right*). In contrast to the dodecamer DNA without drug, the long time component decay with time constants of ≈10 ns (10–20%) is observed for all the transients (from 335 to 440 nm).

The $C(t)$ function in Fig. 4 can be fitted to a biexponential decay with time constants of 0.8 ps (40%) and 10.3 ps (60%); any sub-100-fs components in these dynamics are unresolved. The net spectral shift observed is 574 cm^{-1}, which is smaller than that of the DNA without drug, indicating that the environment around the probe Ap with drug is more nonpolar compared with that in the DNA without drug. The longer time constant in the $C(t)$ is slightly shorter, but its contribution is larger than that for the DNA without drug. The fluorescence anisotropy, $r(t)$, at 380 nm is also persistent, showing a nanosecond decay in the rotational motions, which is consistent with the DNA without drug. In Fig. 5 we show a comparison of the normalized femtosecond-resolved transients (in the blue edge) and hydration correlation functions of the dodecamer, with and without the drug pentamidine, and in bulk water.

The observed ≈80-ps decay component present in the wave-

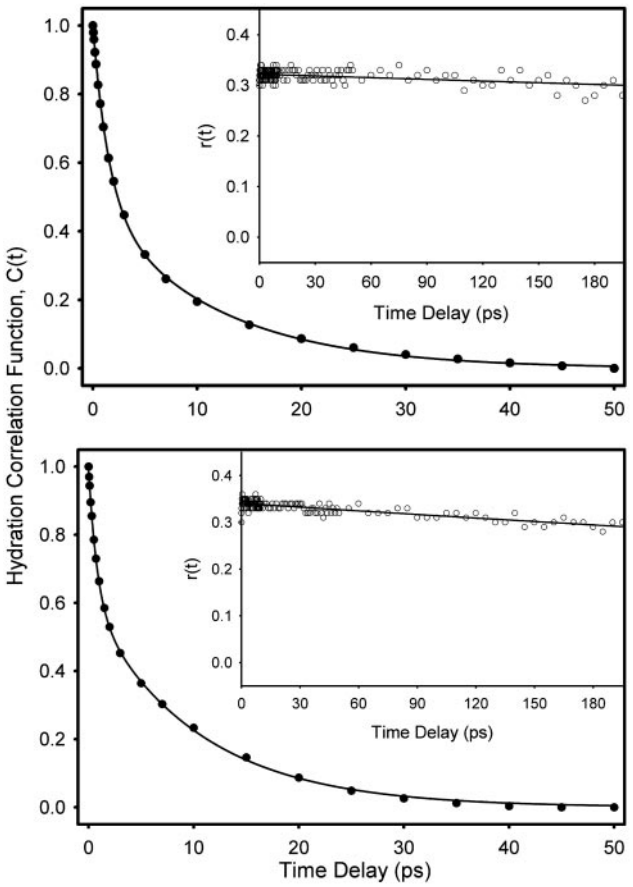

Fig. 4. Hydration correlation function, $C(t)$, of Ap in native dodecamer DNA (*Upper*) and dodecamer DNA–drug complex (*Lower*). (*Insets*) The time-resolved anisotropies, $r(t)$, of Ap in the corresponding systems.

lengths detected, similar to the case without the drug, represents the charge-transfer dynamics of the probe Ap. A recent NMR investigation followed by molecular dynamics simulation has shown that the structural perturbation after binding of the drug pentamidine to the DNA with sequence used in our studies is very small (13). However, the faster decay with a time constant of 80 ps, compared with that in the DNA without drug (150 ps), indicates a favorable stacking of the probe Ap for the charge transfer, after complexation with the drug pentamidine, and possibly the involvement of the drug. Another support for the efficient charge transfer comes from steady-state measurement. The peak intensity of the emission spectrum of the DNA–drug complex is almost half that of the DNA without drug.

Denatured Dodecamer DNA (Single Strand). In 40% formamide aqueous solution (vol/vol), the dodecamer exists as single-stranded DNA (20). Repeating the NMR measurements discussed above for the duplexes in 40% formamide, we did not observe the imino proton signal, consistent with complete denaturation. The steady-state emission for a solution of DNA in 40% formamide (Fig. 2) shows an increase in intensity (6-fold), which is indicative of denaturation and/or solvent effect, as discussed above. However, there is no significant shift of the emission wavelength of the denatured DNA compared with that of the native one. To establish how such formamide concentration alters solvation in the bulk, we studied the dynamics of Ap in solution of the same concentration as a control experiment.

In Fig. 6 *Upper* we show transients obtained from up-conversion experiments on denatured DNA in the 40% formamide solution. The results for the free Ap in the 40% formamide solution are also shown in Fig. 6 *Lower*. The decays for denatured DNA and free Ap in 40% formamide solution are noticeably similar except for the blue end, where the decay shows faster components for denatured DNA compared with those in free Ap. From these transients we constructed $C(t)$ for denatured DNA (Fig. 7 *Upper*) and free Ap in 40% formamide solution (Fig. 6 *Lower*) following the same methodology described above. The $C(t)$ function for denatured DNA can be fitted to a biexponential decay with $\tau_1 = 0.37$ ps (54%) and $\tau_2 = 3.3$ ps (46%). The $C(t)$ function for free Ap in 40% formamide gives $\tau_1 = 1.0$ ps (70%) and $\tau_2 = 3.4$ ps (30%).

The solvation time constants for 40% formamide solution are significantly longer than those observed for free Ap in bulk water without formamide [$\tau_1 = 0.2$ ps (15%) and $\tau_2 = 0.87$ ps (85%)] (ref. 12 and references therein). The change indicates that the

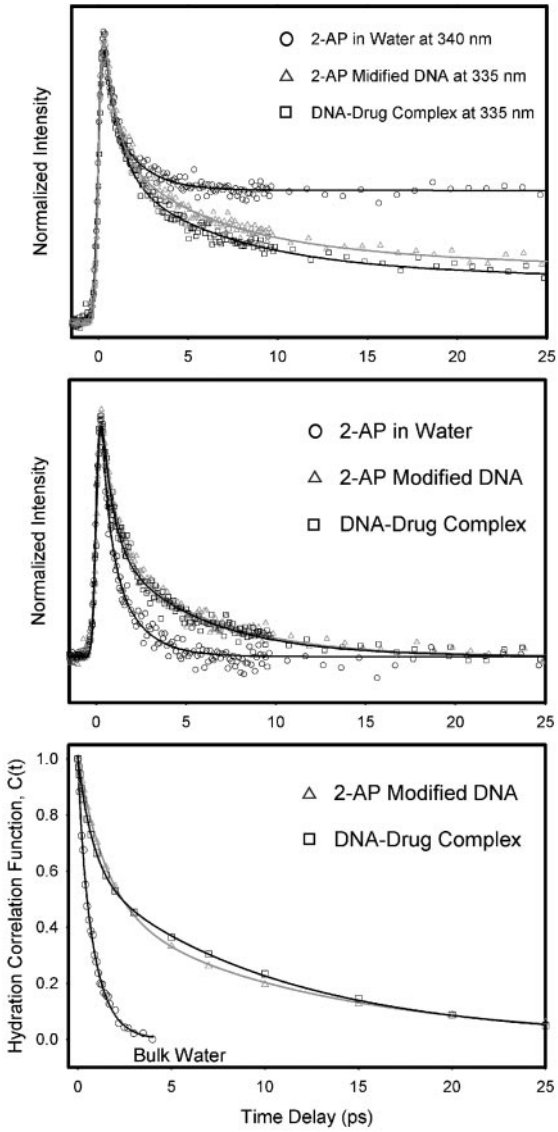

Fig. 5. (*Top*) Normalized femtosecond-resolved fluorescence of the three systems at the emission wavelengths indicated (blue edge of the fluorescence spectra). Note the nanosecond lifetime component in the case of Ap (see text). (*Middle*) The same transients as in *Top*, but after subtracting the long-decay component(s) (see text). (*Bottom*) Comparison of the hydration correlation functions for the dodecamer with and without the drug pentamidine. We also include the results from Ap in bulk water for comparison.

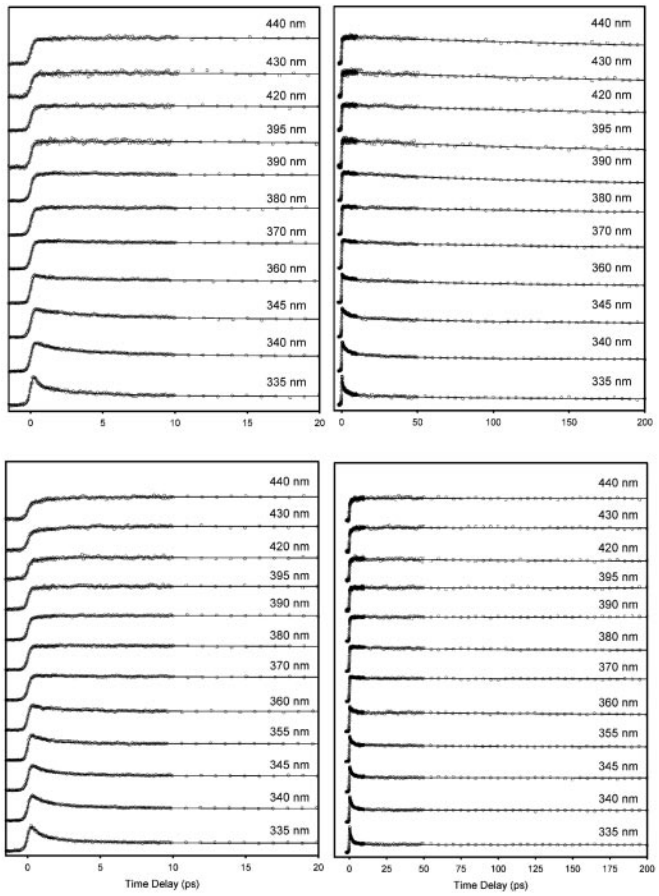

Fig. 6. Femtosecond-resolved fluorescence transients for Ap of denatured dodecamer DNA (*Upper*) and in 40% formamide aqueous solutions (*Lower*). (*Right*) The transients on longer time scales (see text).

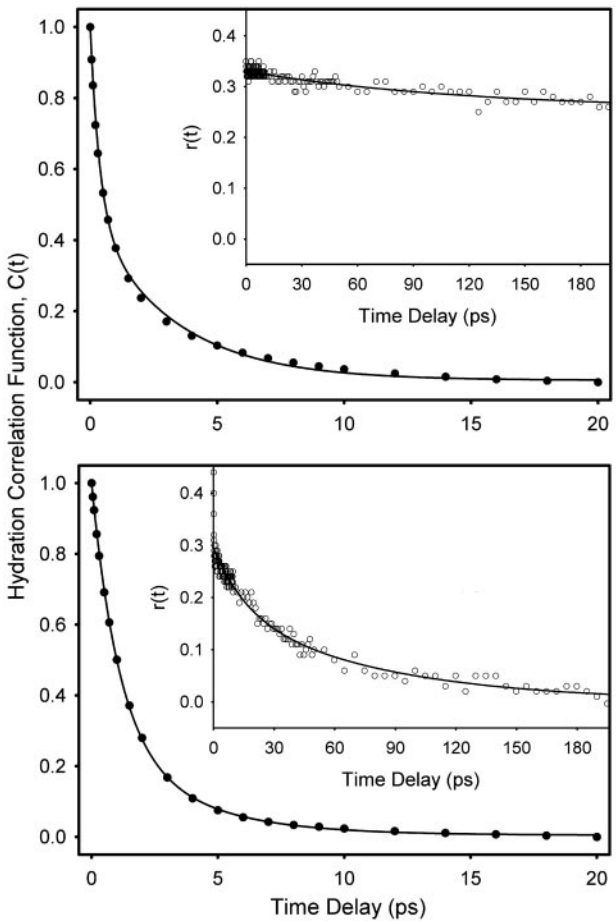

Fig. 7. Hydration correlation function, $C(t)$, of Ap of denatured dodecamer DNA (*Upper*) and in 40% formamide aqueous solutions (*Lower*). (*Insets*) Time-resolved anisotropies, $r(t)$, of Ap in the corresponding systems.

presence of formamide significantly alters solvation dynamics, and the effect must be taken into account when considering the dynamics for denatured DNA. For pure formamide solvent, the correlation function using coumarin as a probe showed a multiexponential behavior (23) with time constants $\tau_1 = 0.03$ ps (8.3%), $\tau_2 = 0.16$ ps (45.4%), $\tau_3 = 2.94$ ps (39.9%), and $\tau_4 = 57.9$ ps (6.4%). Our measured longer time constant of 3.4 ps is in close agreement with one of the major components, 2.94 ps, in pure formamide solution. The faster component ($\approx$1 ps) is close to the longer decay (0.87 ps) in bulk water (ref. 12 and references therein). The variation in time constants most probably is due to selective interactions. Formamide is able to form dimers with water molecules through double hydrogen-bonding (24) as evidenced by microwave spectroscopy (25). The hydrogen-bond breakage of the network also alters the diffusional relaxation (slow component) (26). NMR and molecular dynamics simulation studies have shown recently that formamide is capable of specific interactions with adenine through one to two hydrogen bonds, depending on isomeric conformation of the formamide molecule in the context of a duplex (27).

To probe the local motions of Ap in denatured DNA and in 40% formamide solution, we measured $r(t)$ at 380 nm. In denatured DNA, the anisotropy (Fig. 7 *Upper Inset*) is persistent up to 200 ps with a large constant value of 0.26. The early decay component of 120 ps (23%) results from local motion in the absence of stacking. The persistence of the anisotropy indicates that no large amplitude diffusive motion is present, and Ap is essentially "frozen" in denatured DNA on this time scale. In contrast, the $r(t)$ of Ap in 40% formamide solution (Fig. 7 *Lower Inset*) shows two decay components with time constants of 16 ps (38%) and 77 ps (62%), and the final anisotropy decays to nearly zero. Hence, the local restriction of Ap in denatured DNA is not due to the viscosity of the denaturing solvent.

To investigate the effect of attachment of deoxyribose sugar moiety to the Ap fluorophore in the DNA, which is absent in the free Ap used in the study mentioned above, we measured the anisotropy of deoxyribose-Ap in bulk water (Fig. 8 *Upper*); the time constants of the $r(t)$ decay are 23 ps (52%) and 82 ps (48%). The $r(t)$ of Ap in water is shown in Fig. 8 *Lower*; the time constants are 19 ps (58%) and 54 ps (42%). The decay profile of the $r(t)$ of deoxyribose-Ap is not much different from that of the free Ap in water or denaturing solvent; the presence of a small (120-ps) decay in the $r(t)$ of denatured DNA (single strand) suggests a certain degree of flexibility. The rigidity of the probe Ap in DNA single strands is not from the hydrogen-bonding with other strands as evidenced by our NMR measurements, discussed above. Thus, it is the anchoring of the Ap molecule to the DNA backbone, as an integral part of the phosphate-sugar-base, that restricts its motion. This restriction should be significant in the efficiency of forming double-stranded helical DNA.

The effect of unstacking on the electron transfer is reflected in the decay times of transients. A decay component of time constants $\approx$300 ps is present when comparing the red-edge transients of native and denatured DNA (Figs. 3 and 6). In addition, the $\approx$10-ns decay component, which is the lifetime of the relaxed Ap molecule, increases in its contribution, up to 50% (Fig. 6) in the red end. The lengthening of the decay time constant in the denatured DNA

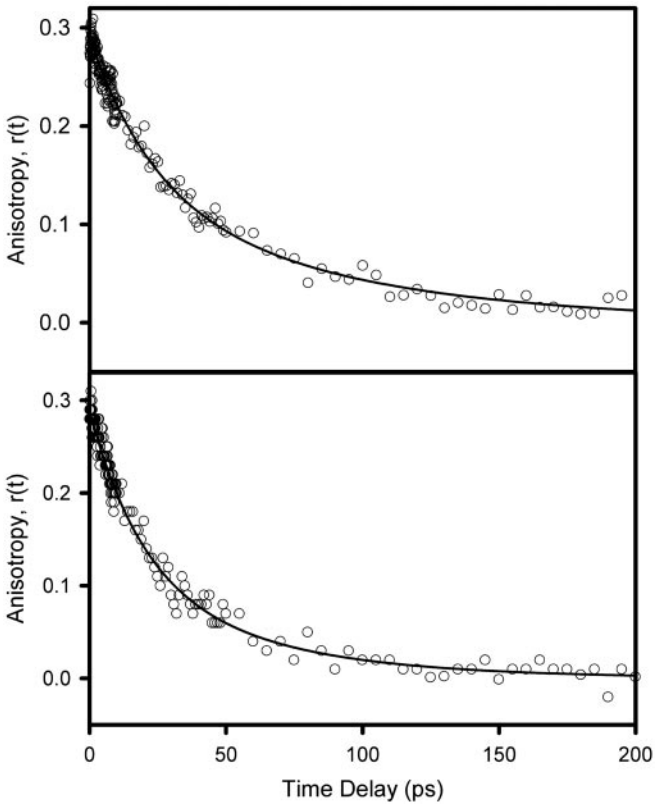

Fig. 8. Anisotropy *r*(*t*) of the probes deoxyribose-Ap (*Upper*) and free Ap (*Lower*) in water.

(≈300 ps) compared with those in native DNA duplex (≈150 ps) and DNA–drug complex (≈80 ps) and the increased contribution of the 10-ns decay component from ≈10–20% to ≈50% indicate less efficient electron transfer when stacking is disrupted. Residual interactions of Ap with neighboring bases are caused by the rigidity in the assembly. A complete loss of rigidity will occur on a time scale much longer than those discussed above.

Major and Minor Groove Hydration. Hydration dynamics in the DNA grooves using the intrinsic Ap, a mimic of natural DNA purine bases, characterize the time scales involved with femtosecond resolution. The probing of the dynamics made here is without spatial averaging and for a prescribed sequence. The omnipresence of water molecules in the grooves is clearly demonstrated. The separation of time scale of hydration (≈12 ps) from that of electron transfer (≈150 ps) in the case of native DNA allowed us to measure water dynamics inside the grooves without major interference from the latter process. The labeling position of A5 (between two adenines) was chosen strategically to avoid efficient electron transfer involving neighboring G or C [≈20 ps (17)] bases. Two types of trajectories of hydration have been observed, bulk type and layer type; both are dynamically involved. In the native DNA, the probe Ap is relatively rigid and restricted in motion in the DNA as evidenced by its anisotropy decay; however, the water reorientation in the network is what determines the rigidity and order of the layer.

Hydration dynamics observed in the Ap-modified DNA duplex and the DNA–drug complex (10–12 ps) is 2-fold faster than that observed for DNA with drug (Hoechst 33258) in the minor groove (≈20 ps) (8). In that study, we probed water dynamics in the minor groove because the drug (Hoechst 33258) was the excited dipole, and it is certain that the drug is in the minor groove. In this study, Ap is positioned on the floor of two grooves; i.e., it interfaces with both major and minor grooves, and Ap is the excited dipole, in the presence or absence of the drug (pentamidine). For both the DNA and the DNA–drug complex, a significant number of water molecules from the major groove dominate hydration dynamics of Ap. However, water molecules in the major groove of DNA are less ordered, (i.e., more bulk type) than those in the minor groove on the NMR time scale (19). Recent molecular dynamics simulations of ultrafast hydration in 16-mer duplex DNA found no significant difference between major and minor groove hydration. The time scale is consistent with our measurements: the average residence time was found to vary from 11 to 18 ps with a maximum of ≈200 ps; layer thickness changes these numbers (28).

The long residence time (nanoseconds) of water molecules detected by NMR (19) is more important for maintaining the structural integrity (structural water), whereas the dynamically ordered water is of more significance to recognition processes such as those involved in ligand (29) or protein (30) binding. The high mobility of water at the interface is critical to the net entropy change of recognition and to making a layer of "lubricant" for improving complementarity of recognition by virtue of its almost bulk-like property.

This work was supported by the National Science Foundation.

1. Westhof, E. (1988) *Ann. Rev. Biophys. Chem.* **17,** 125–144.
2. Halle, B. & Denisov, V. P. (1998) *Biopolymers* **48,** 210–233.
3. Cheatham, T. E., III, & Kollman, P. A. (2000) *Annu. Rev. Phys. Chem.* **51,** 435–471.
4. Chalikian, T. V., Volker, J., Srinivasan, A. R., Olson, W. K. & Breslauer, K. J. (1999) *Biopolymers* **50,** 459–471.
5. Woda, J., Schneider, B., Patel, K., Mistry, K. & Berman, H. M. (1998) *Biophys. J.* **75,** 2170–2177.
6. Robinson, C. R. & Sligar, G. (1993) *J. Mol. Biol.* **234,** 302–306.
7. Rand, R. P. (1992) *Science* **256,** 618.
8. Pal, S. K., Zhao, L. & Zewail, A. H. (2003) *Proc. Natl. Acad. Sci. USA* **100,** 8113–8118.
9. Sowers, L. C., Fazakerley, G. V., Eritja, R., Kaplan, B. E. & Goodman, M. F. (1986) *Proc. Natl. Acad. Sci. USA* **83,** 5434–5438.
10. Law, S. M., Eritja, R., Goodman, M. F. & Breslauer, K. J. (1996) *Biochemistry* **35,** 12329–12337.
11. Edwards, K. J., Brown, D. G., Spink, N., Skelly, J. V. & Neidle, S. (1992) *J. Mol. Biol.* **226,** 1161–1173.
12. Pal, S. K., Peon, J. & Zewail, A. H. (2002) *Chem. Phys. Lett.* **363,** 57–63.
13. Jenkins, T. C., Lane, A. N., Neidle, S. & Brown, D. G. (1993) *Eur. J. Biochem.* **213,** 1175–1184.
14. Edwards, K. J., Jenkins, T. C. & Neidle, S. (1992) *Biochemistry* **31,** 7104–7109.
15. Matesoi, D., Kittler, L., Bell, A., Unger, E. & Lober, G. (1996) *Biochem. Mol. Biol. Int.* **38,** 123–132.
16. Pal, S. K., Peon, J. & Zewail, A. H. (2002) *Proc. Natl. Acad. Sci. USA* **99,** 15297–15302.
17. Wan, C., Fiebig, T., Schiemann, O., Barton, J. K. & Zewail, A. H. (2000) *Proc. Natl. Acad. Sci. USA* **97,** 14052–14055.
18. Fiebig, T., Wan, C. & Zewail, A. H. (2002) *Chemphyschem* **3,** 781–788.
19. Lane, A. N., Jenkins, T. C. & Frenkiel, T. A. (1997) *Biochim. Biophys. Acta* **1350,** 205–220.
20. Sambrook, J. & Russell, D. W. (2001) *Molecular Cloning: A Laboratory Manual* (Cold Spring Harbor Lab. Press, Plainview, NY).
21. Holmén, A., Nordén, B. & Albinsson, B. (1997) *J. Am. Chem. Soc.* **119,** 3114–3121.
22. Jean, J. M. & Hall, K. B. (2002) *Biochemistry* **41,** 13152–13161.
23. Horng, M. L., Gardecki, J. A., Papazyan, A. & Maroncelli, M. (1995) *J. Phys. Chem.* **99,** 17311–17337.
24. Fu, A., Du, D. & Zhou, Z. (2003) *J. Mol. Struct.* **623,** 315–325.
25. Lovas, F. J., Suenram, R. D. & Fraser, G. T. (1988) *J. Chem. Phys.* **88,** 722–729.
26. Bhattacharyya, S. M., Wang, Z.-G. & Zewail, A. H. (2003) *J. Phys. Chem.*, in press.
27. Maufrais, C. & Boulard, Y. (2002) *Can. J. Physiol. Pharmacol.* **80,** 609–617.
28. Bonvin, A. M., Sunnerhagen, M., Otting, G. & van Gunsteren, W. F. (1998) *J. Mol. Biol.* **282,** 859–873.
29. Chalikian, T. V., Plum, G. E., Sarvazyan, A. P. & Breslauer, K. J. (1994) *Biochemistry* **33,** 8629–8640.
30. Billeter, M., Guntert, P., Luginbuhl, P. & Wuthrich, K. (1996) *Cell* **87,** 1057–1065.